

Influence of pressure on the energy spectrum of ruthenium

E. S. Alekseev, V. A. Venttsel', O. A. Voronov, A. I. Likhter, and M. V. Magnitskaya

Institute of High-Pressure Physics, Academy of Sciences of the USSR, Akadengorodok, Moscow Province

(Submitted 21 June 1978)

Zh. Eksp. Teor. Fiz. 76, 215–222 (January 1979)

Measurements of the de Haas–van Alphen effect under pressures up to 2 kbar were used in a study of the β and γ sections of the Fermi surface in magnetic fields oriented along the principal crystallographic directions. The augmented plane wave method was employed in a calculation of the energy spectrum of conduction electrons. The calculation and experimental values were used to determine the Fermi energy and its pressure dependence.

PACS numbers: 71.25.Hc, 62.50.+p

1. INTRODUCTION

We shall describe a theoretical and experimental investigation of the energy spectrum of ruthenium. Ruthenium has the hcp lattice with the parameters $a_{\text{lat}} = 2.704 \text{ \AA}$ and $c_{\text{lat}} = 4.276 \text{ \AA}$ at 4.2°K (Ref. 1). The Brillouin zone of this lattice is a hexagonal prism with the parameters $a = 1.549 \text{ \AA}^{-1} = 0.8197 \text{ a.u.}$, $b = 1.469 \text{ \AA}^{-1} = 0.7773 \text{ a.u.}$ The Fermi surface of ruthenium was investigated by Coleridge, who used the de Haas–van Alphen effect method in pulsed² and static³ magnetic fields; the linearized muffin-tin orbital (LMTO) method was used by Jepsen *et al.*⁴ to calculate the energy spectrum of ruthenium under equilibrium volume conditions. Figure 1 shows the Fermi surface based on the results of Refs. 2–4 and on the calculations reported below. The orbit notation in Fig. 1 agrees with the designations of the oscillation frequencies in Ref. 3.

The seventh energy zone contains two groups of hole ellipsoids, one of which is located approximately at the midpoint of the LM line (β orbits) and the other surrounds the points L in the Brillouin zone (α orbits). The dimensions of these ellipsoids are small and the associated oscillation frequencies lie within a range corresponding to $(0.3\text{--}2.0) \times 10^7 \text{ Oe}$.

The eighth zone contains a complex multiply connected monster surface, which—in the extended band scheme—has open directions along the $[0001]$ axis and at right-angles to this axis. The frequencies λ and ω are associated with the monster surface.

The ninth energy zone contains a roughly spherical electron surface flattened along the $[0001]$ axis; this surface surrounds the point Γ in the Brillouin zone and it resembles a squash. The frequencies σ , τ , and ρ are associated with this squash surface.

In the tenth energy zone there is another roughly spherical electron surface with a void in its middle; it surrounds the point Γ and resembles a flattened ripe plum from which the stone has been removed. The orbits passing on the outer side of the plum are associated with the frequencies ν and μ and the orbit passing inside the void is associated with the frequency γ .

The frequency γ is of the same order of magnitude as the frequencies α and β , whereas the other frequencies are an order of magnitude higher: they correspond to $(10\text{--}20) \times 10^7 \text{ Oe}$.

The structure factor for the ALH faces is zero and, therefore, on these faces the energy zones 7 and 8, as well as 9 and 10, are separated in pairs by just a narrow spin–orbit gap. This gap vanishes along the line AL and, therefore, degeneracy along this line is not lifted.

The magnetic-field dependences of the oscillation amplitudes for the α orbits³ and of the magnetoresistance⁵ indicate the occurrence of magnetic breakdown (breakthrough) between the monster and a pocket α , separated by a narrow spin–orbit gap. The resultant magnetic-breakdown orbit λ is shown in Fig. 1. The large parts of the Fermi surface (the monster, squash, and plum) have a fairly complex shape, whereas the small parts associated with the sections α , β , and γ are very close to ellipsoids, as confirmed by the angular dependences of the areas of their external sections. A calculation of these areas is thus simplified because it is sufficient to know the principal axes of the ellipsoids.

Measurements of the influence of pressure on the Fermi surface of ruthenium are difficult because of its low compressibility [$d(\ln V)/dp = -0.317 \times 10^{-3} \text{ kbar}^{-1}$], which is almost the same along the hexagonal axis [$d(\ln c)/dp = -0.099 \times 10^{-3} \text{ kbar}^{-1}$] and at right-angles to this axis [$d(\ln a)/dp = -0.109 \times 10^{-3} \text{ kbar}^{-1}$] (Ref. 6). The dependence of the area of the extremal section γ in the $H \parallel [0001]$ case is⁷ $d(\ln S_\gamma)/d(\ln V) = -1 \pm 0.1$. A short note⁸ reports the results of a study of the pressure dependence of the extremal section γ for the three principal directions of the magnetic field and it shows that in the $H \parallel [0001]$ case the value of $d(\ln S_\gamma)/dp = (0.3 \pm 0.02) \times 10^{-3} \text{ kbar}^{-1}$ agrees with the results of Ref. 7, whereas

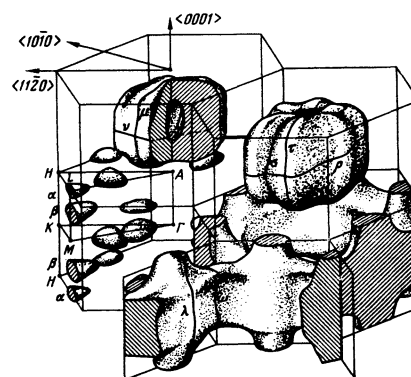


FIG. 1. Fermi surface of ruthenium.

in the $H \perp [0001]$ case this quantity is $d(\ln S_p)/dp = -(0.34 \pm 0.02) \times 10^{-3} \text{ kbar}^{-1}$.

2. EXPERIMENTAL METHOD AND RESULTS

We used the modulation method of recording the de Haas-van Alphen effect⁹ in a static field generated by a superconducting solenoid. The change in the oscillation frequency under the influence of pressure was deduced from the phase shift of the oscillations¹⁰

$$\frac{d \ln F}{dp} = \frac{1}{p} \frac{\Delta \varphi}{2\pi F} H$$

The apparatus was described in Refs. 8 and 11.

In view of the low and almost isotropic compressibility of ruthenium the phase shift $\Delta \varphi$ of the oscillations at pressures transmitted by liquid helium amounted to just a few degrees, which was comparable with the error in the determination of the phase shift and limited the precision of the pressure coefficient $d(\ln S)/dp$ to ~50%. Employing pressures up to 3 kbar transmitted by solid helium¹² it was possible to increase considerably the phase shift and, consequently, improve the precision of the determination of the pressure coefficient. Pressure was established at room temperature and the vessel was cooled slowly under constant pressure until helium solidified; the subsequent cooling occurred under constant-volume conditions. The reduction in pressure as a result of cooling of solid helium was deduced from the results of Ref. 13 and was monitored on the basis of the change in the oscillation frequency of cadmium reported in Ref. 14. In the case of ruthenium the oscillation phase for the β and γ cross sections changed by π at pressures of 1–2 kbar and a further increase in the pressure was pointless. When solid helium was used, the error in the determination of the phase shift $\Delta \varphi$ was $\leq 1\%$ and, therefore, the main error in the pressure coefficient resulted from inaccuracy of the pressure measurements.

During slow freezing of helium the oscillation amplitude decreased by a factor not exceeding 1.5, compared with the oscillation amplitude at atmospheric pressure, and was restored completely on reduction in pressure. There was no reduction either in the oscillation amplitude after many cycles in which pressure was increased and lowered. All this indicated that the pressure was close to hydrostatic.

Measurements were carried out on ruthenium samples $[R(300 \text{ K})/R(4.2 \text{ K} \approx 1200)]$ of $0.5 \times 0.5 \times 5 \text{ mm}$ dimensions elongated along the $[0001]$, $[10\bar{1}0]$, and $[11\bar{2}0]$ axes; these samples were clamped rigidly inside the channel of a high-pressure bomb thus avoiding the possibility of changes in the orientation of the sample during the application of pressure. The oscillations were recorded three times: at atmospheric pressure, under a high pressure, and after removal of high pressure. The bomb was subjected to the field of a short-circuit superconducting solenoid and the magnetic field scanning ($\sim 500 \text{ Oe}$) was provided by a magnetization coil which was not coupled electrically to the modulation coil. Energy dissipation in the ohmic resistance of the superconducting shunt reduced the magnetic field in a

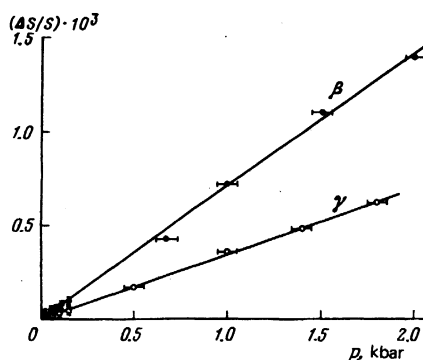


FIG. 2. Dependence of the relative change in the area of extremal sections of the ellipsoids γ and β on the pressure in $H \parallel [10\bar{1}0]$.

short-circuited solenoid at a rate of $\sim 3 \text{ Oe/h}$, which resulted in a considerable reduction of the "frozen in" field during experiments lasting 5–6 h. This reduction in the field was allowed for carefully in the analysis of the results.

Oscillations of the susceptibility were recorded at the n -th harmonic of the modulation frequency and the value of n was selected to range from 2 to 12 so as to separate, if possible, the oscillations associated with the various parts of the Fermi surface. Similar oscillation frequencies associated with the sections β and γ (in the $H \parallel [11\bar{2}0]$ case, these were $F_\beta = 1.3 \times 10^7 \text{ Oe}$ and $F_\gamma = 1.41 \times 10^7 \text{ Oe}$) were separated by selecting the modulation amplitude only for some orientations of the samples; in this case the oscillations recorded on punched tape represented a superposition of two frequencies. An analysis of the results on a computer involved accurate determination of the phase shift of the oscillations at each of the frequencies.

The pressure coefficients $d(\ln S)/dp$ were obtained for the sections β and γ . The dependence of $\Delta S/S$ on p is shown for these sections in Fig. 2 and the coefficients for the three principal directions in the crystal are listed in Table I.

The oscillations associated with the section α are of amplitude which is almost three orders of magnitude less than the oscillations associated with the sections β and γ . This is due to the fact that the section α may be observed only in weak fields as long as the magnetic breakdown between the section α and the monster is difficult. The high-frequency oscillations have a simi-

TABLE I. Logarithmic pressure derivatives $[d(\ln S)/dp] \times 10^3$ (kbar^{-1}) of extremal sections.

H	α	β	β'	γ	ρ	ν
Experimental data						
$[10\bar{1}0]$	—	0.72 ± 0.08	0.72 ± 0.25	0.34 ± 0.02	—	—
$[11\bar{2}0]$	—	0.68 ± 0.20	0.69 ± 0.25	0.34 ± 0.02	—	—
$[0001]$	—	0.70 ± 0.20	—	0.30 ± 0.02	—	—
APW calculations						
$[10\bar{1}0]$	-1.1	-0.23	-0.18	-0.15	0.70	0.78
$[11\bar{2}0]$	-1.0	-0.12	-0.22	-0.48	0.74	0.68
$[0001]$	-0.18	0.094	—	-0.93	0.62	0.38
Calculations based on experimental data						
$[10\bar{1}0]$	1.8	1.22 ± 0.2	1.05	0.43 ± 0.2	0.085	0.18
$[11\bar{2}0]$	1.8	0.88 ± 0.2	1.16	0.43 ± 0.2	0.11	0.10
$[0001]$	0.94	0.99 ± 0.2	—	0.36 ± 0.2	0.26	0.08

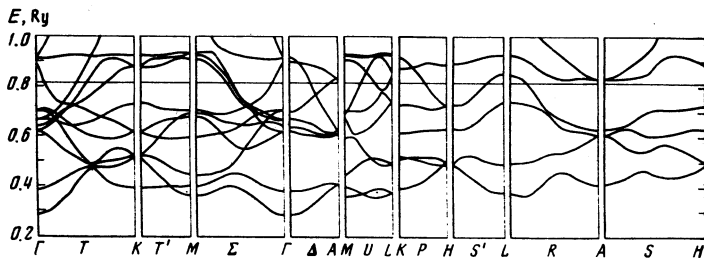


FIG. 3. Energy spectrum of ruthenium.

lar small amplitude but this is due to the fact that the fields up to 50 kOe, used in our experiments, are too low for reliable recording of the oscillations and their phase shift under pressure because the orbits associated with these sections correspond to very large effective masses ($m^*/m_0 \sim 1.2-2.0$).

3. ANALYSIS OF RESULTS

A. Calculation of the energy band structure

The energy spectrum of conduction electrons was calculated by the augmented plane wave (APW) method. This was done to help in the interpretation of the experimental frequency spectra deduced from the de Haas-van Alphen effect in ruthenium and their pressure dependences, and to check the correctness of the Fermi surface model. The calculations were carried out for two volumes corresponding to $p=0$ and $p=100$ kbar in the case when the compressibility coefficient was linear. The large difference between the volumes, compared with those under the pressures used in our experiments, was selected so that the changes in the energy spectrum exceeded the precision of the calculations and made it possible to compare the theoretical values of the logarithmic derivatives of the Fermi surface sections with the experimental ones. The calculations were linked to the experimental results at $p \leq 2$ kbar by assuming arbitrarily that the elastic constants were independent of pressure and all the changes in the areas of the extremal sections were reduced to the pressure of $p=1$ kbar. The calculations were carried out by the Slater asymmetric APW method¹⁵ and the muffin-tin (MT) potential was formed by superposing the exchange potential in the Slater approximation and the screened Coulomb potential. The atomic wave functions for the electron density calculations were taken from the tables of Herman and Skillman.¹⁶ The crystal potential curves were plotted allowing for the contribution of the neighboring atoms in the first 14 coordination spheres.

Expansion of an augmented plane wave in terms of spherical harmonics was made using 12 terms ($l=12$) and the test function was a combination of 37 APW's. In both cases the MT radius was calculated from the condition of tangency of the MT spheres.

The calculations were carried out at the high-symmetry points and along the high-symmetry directions of the irreducible part, representing 1/24-th of the Brillouin zone. The results of calculations of the energy band structure of ruthenium are presented in Fig. 3. Qualitatively, the calculated band structure is in

agreement with the results of calculations of Jepsen *et al.*,⁴ so that we can regard as reliable the form of the Fermi surface (Fig. 1) deduced from theoretical calculations carried out in the present paper and by Jepsen *et al.*⁴

B. Calculation of the Fermi level

As in the work of Kulikov and Kuz'min,¹⁷ the Fermi level was determined from 12 representative points in the irreducible part of the Brillouin zone; the coordinates of the representative points were given in Ref. 18. Energy was measured from the minimum of the first band. Its value from the MT zero was as follows for the two selected volumes: $E(0)=0.2875$ Ry and $E(100 \text{ kbar})=0.3122$ Ry.

The precision of determination of the Fermi level ϵ_F by the APW calculations did not exceed 0.01 Ry, but this was sufficient for a qualitative description of the Fermi surface. However, such precision was unsatisfactory in the calculation of the derivatives with respect to pressure, which would agree with the experimental data. Therefore, the Fermi energy was determined also empirically, namely so as to fit best the experimental results on the section γ for field directions along the principal crystallographic axes. Then, the selected values $\epsilon_F(0)$ and $\epsilon_F(p)$ were checked for all the other Fermi surface sections in the ellipsoidal approximation. Figure 4 shows the branches of the energy spectrum near the Fermi surface governing the axes of the

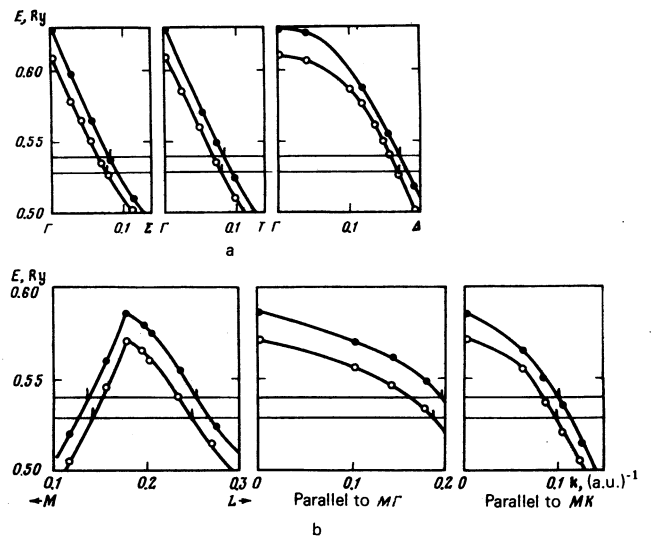


FIG. 4. Energy spectrum of ruthenium near the Fermi energy: a) γ ellipsoid; b) β ellipsoid; \circ) $p=0$; \bullet) $p=100$ kbar. The horizontal lines show the values of $\epsilon_F^{(2)}$ adjusted in accordance with the experimental data.

TABLE II. Areas of extremal sections S (a.u.) of Fermi surface of ruthenium.

H	α	β	β'	γ	ρ	ν
Experimental data						
[1010]	0.0093	0.0200	0.0290	0.0373	0.475	0.384
[1120]	0.0120	0.0347	0.0230	0.0376	0.501	0.408
[0001]	0.0267	0.0547	—	0.0213	0.576	0.421
APW calculations						
[1010]	0.026	0.025	0.0363	0.054	0.384	0.288
[1120]	0.025	0.046	0.0273	0.054	0.380	0.335
[0001]	0.075	0.072	—	0.028	0.533	0.440
Calculations based on experimental data						
[1010]	0.013	0.0162	0.0247	0.0417	0.452	0.343
[1120]	0.012	0.0327	0.0180	0.0417	0.450	0.399
[0001]	0.053	0.0538	—	0.0196	0.586	0.484

β and γ ellipsoids. The positions of $\epsilon_F(0)$ and $\epsilon_F(p)$ were selected in such a way as to make the areas of three sections S_γ closest to those found experimentally, and the values of $\Delta S/\rho S$ closest to the measured pressure coefficients; the adjustment was made by the least-squares method.

Table I lists not only the experimental values of $d(\ln S)/dp$ but also the results of calculations of the logarithmic derivatives of the sectional areas with respect to pressure, found using the energy band structure (Fig. 3) and the values of the Fermi energy deduced by the APW method ($\epsilon_F^{(1)}$) and by adjustment to the γ sections ($\epsilon_F^{(2)}$). The absolute areas of the extremal cross sections calculated by both methods are listed in Table II, together with the experimental data.³ It should be pointed out that the ellipsoidal approximation for the α , ρ , and ν orbits is rough and, therefore, a comparison of these areas is purely illustrative. For the β sections lying on other faces of the Brillouin zone and rotated by 60° about the [0001] axis relative to the principal β section, the calculations of S and $d(\ln S)/dp$ were carried out in the ellipsoidal approximation. These sections are denoted by β' in Tables I and II.

Table III gives the Fermi energies $\epsilon_F^{(1)}$ and $\epsilon_F^{(2)}$, as well as their pressure dependences. For comparison, this table gives the values of $-(\frac{2}{3})d(\ln V)/dp$, which correspond to $d(\ln \epsilon_F)/dp$ if the change in ϵ_F is entirely due to the change in the Brillouin zone volume.

The data in Tables I and II make it clear that the selected value of $\epsilon_F^{(2)}$ agrees with the experimental data for all the Fermi surface sections and the dependence $\epsilon_F^{(2)}(p)$ deduced from the experimental results for the section γ ensures a satisfactory agreement between the calculated and experimental values of $d(\ln S)/dp$ for the β and β' sections.

The calculated energy $\epsilon_F^{(1)}$ usually gives a slightly poorer fit to the areas of the extremal sections and the incorrect sign of their pressure dependences. This is to be expected because the changes in $\epsilon_F^{(1)}$ under pressure are comparable with the error in the determination of ϵ_F from the density of states.

We can thus see that experimental data on some parts

TABLE III. Fermi energies and their pressure derivatives.

	ϵ_F , Ry	$\frac{d \ln \epsilon_F}{dp} \cdot 10^4$, kbar ⁻¹	$-\frac{2}{3} \frac{d \ln V}{dp} \cdot 10^4$, kbar ⁻¹
APW calculation	0.515	0.29	0.21 [4]
Calculations based on experimental data	0.528	0.23±0.01	—

of the Fermi surface along different directions of the magnetic field, on the one hand, and calculations of the energy spectra for two volumes, on the other, allow us to conclude that the model description of the Fermi surface of ruthenium is not in conflict with the influence of pressure on this surface. A comparison of the theory with the experimental data makes it possible to find the exact change in the Fermi energy under pressure, which follows from this model and which is difficult to find theoretically because of the special nature of the calculations of the Fermi energy and errors in such calculations.

The authors are deeply grateful to R. G. Arkhipov for discussing the results and A. V. Rudnev for valuable consultations, and also to N. V. Volkenshtein and V. E. Startsev for their interest and valuable advice.

- ¹E. O. Hall and J. Crangle, Acta Crystallogr. 10, 240 (1957).
- ²P. T. Coleridge, Phys. Lett. 22, 367 (1966).
- ³P. T. Coleridge, J. Low Temp. Phys. 1, 577 (1969).
- ⁴O. Jepsen, O. K. Andersen, and A. R. Mackintosh, Phys. Rev. B 12, 3084 (1975).
- ⁵V. E. Startsev, V. P. Dyakina, and N. V. Volkenshtein, Pis'ma Zh. Eksp. Teor. Fiz. 23, 43 (1976) [JETP Lett. 23, 38 (1976)].
- ⁶E. S. Fisher and D. Dever, Trans. Metall. Soc. AIME 239, 48 (1967).
- ⁷I. V. Svechkarev, V. B. Pluzhnikov, N. V. Volkenshtein, V. E. Startsev, and V. V. Boiko, Phys. Status Solidi B 55, K5 (1973).
- ⁸V. A. Venttsel', O. A. Voronov, and A. I. Likhter, Fiz. Met. Metalloved. 46, 430 (1978).
- ⁹D. Shoenberg and P. J. Stiles, Proc. R. Soc. London Ser. A 281, 62 (1964).
- ¹⁰I. M. Templeton, Proc. R. Soc. London Ser. A 292, 413 (1966).
- ¹¹V. A. Venttsel', O. A. Voronov, A. I. Likhter, and A. V. Rudnev, Zh. Eksp. Teor. Fiz. 65, 2445 (1973) [Sov. Phys. JETP 38, 1220 (1974)].
- ¹²J. S. Dugdale and J. A. Hulbert, Can. J. Phys. 35, 720 (1957).
- ¹³J. S. Dugdale and F. E. Simon, Proc. R. Soc. London Ser. A 218, 291 (1953).
- ¹⁴V. A. Venttsel', O. A. Voronov, A. I. Likhter, and A. V. Rudnev, Zh. Eksp. Teor. Fiz. 70, 272 (1976) [Sov. Phys. JETP 43, 141 (1976)].
- ¹⁵L. F. Mattheiss, J. H. Wood, and A. Switendick, in: Methods in Computational Physics, Vol. 8, Energy Bands of Solids (ed. by B. Alder, S. Fernbach, and M. Rotenberg), Academic Press, New York (1968), p. 63.
- ¹⁶F. Herman and S. Skillman, Atomic Structure Calculations, Prentice-Hall, Englewood Cliffs, N.J., 1963.
- ¹⁷N. I. Kulikov and Yu. M. Kuz'min, Izv. Vyssh. Uchebn. Zaved. Chern. Metall. No. 9, 113 (1977).
- ¹⁸D. J. Chadi and M. C. Cohen, Phys. Rev. B 8, 5747 (1973).

Translated by A. Tybulewicz